Geo-electrical structure of the mantle beneath the Indian region derived from the 27-day variation and its harmonics

E. Chandrasekhar*

Research Centre for Earthquake Prediction, Disaster Prevention Research Institute, Kyoto University, Gokasho, Uji 611-0011, Kyoto, Japan

Estimates of the C-response function were determined by $Z : H$ method to obtain conductivity and depth values for a substitute perfect conductor (conductosphere) beneath the Indian region, utilizing geomagnetic variations at periods of 27-day and its harmonics. Two and half years of continuous geomagnetic data were utilized. These data were recorded during 1975–77, at a chain of 13 stations confined to the 150^0 geomagnetic longitude band, which extended from the dip-equator at the southern tip of India, to the northern parts of Russia. Complex demodulation technique was employed to determine the electromagnetic (EM) responses. Taking advantage of the dense latitudinal distribution of the observatories, the demodulates of all the stations were tested statistically to check the validity of the P_1^0 approximation for the inducing field. Single-station response estimates, for a 27-day period, computed by a robust method have shown that reliable EM responses (consistent with P_1^0 source dependence and with local 1-D Earth structure) could be obtained for only 6 stations, all situated in the mid-latitude region. The depth estimates at all 6 stations are consistent, including Sabhawala (SAB) which is situated close to the Himalayan collision zone. The negligible differences in the depth estimates of these mid-latitude stations do not show any latitudinal dependence, as against such an observation reported for the European and the North American regions. The mean depth of the conductosphere is found to be 1200 ($\pm$200) km, with an average conductivity of 0.7 ($\pm$0.3) S/m. Comparison of the mean geo-electrical structure with those of other regional models shows that the presence of a mid-mantle conductor at 850 km depth could be considered to be a global phenomenon.

1. Introduction

A successful determination of the mantle conductivity distribution using long-period geomagnetic variations essentially depends on (i) *a priori* knowledge of the spatial structure of the inducing field and (ii) the nature of the local 1-D internal structure of the Earth. The spatial structure of such long-period (>3–4 days) variations of global origin, generated by a symmetric magnetospheric ring current, can adequately be represented by a single P_1^0 zonal harmonic term (Chapman and Price, 1930; Banks, 1969). At equatorial and auroral regions, since the field variations are largely contaminated due to the effects of equatorial and auroral electrojets, the P_1^0 zonal approximation of the inducing source may not be valid. However, at mid-latitude regions, a zonal representation of the external source generally holds good. Thus, Schultz and Larsen (1987) in their global induction study showed that an electromagnetic (EM) response, consistent with both a P_1^0 nature for the inducing source and a local 1-D Earth structure, could be determined only for stations situated in the mid-latitude region. Banks and Ainsworth (1992), by analyzing hourly mean values of two years of continuous data from as many as 130 observatories worldwide, confirmed the dominance of the P_1^0 term in the spatial representation of long-period variations in mid-latitude regions. Chandrasekhar and Arora (1992), by establishing source-field characteristics, determined upper mantle conductivity information for the region under study in the present paper, using geomagnetic storm-time variations. Recently, Honkura and Matsushima (1998), while determining a global mantle conductivity distribution using 10 years of data from 59 observatories, showed that the validity of the P_1^0 approximation generally holds good for geomagnetic variations at long periods, except for annual and semi-annual variations.

In an attempt to provide more information on the mantle conductivity distribution of the Indian region, the present work (a sequel to our earlier study, Chandrasekhar and Arora, 1996), has been undertaken with special attention given to lateral conductivity contrasts at lower mantle depths. This objective is accomplished by determining robust single-station EM responses, following a statistical test for the validity of the P_1^0 character of the data. Depth estimates obtained for 27-day period are discussed in the light of their dependency with latitude, and compared with earlier results (Pecova *et al.*, 1980; Petersons and Anderssen, 1990). After augmenting the response estimates with those of Sq analysis obtained from the same data sets, the geo-electrical structure for the Indian region is discussed and compared with other regional models.

*On leave from Indian Institute of Geomagnetism, Colaba, Mumbai-5, India.

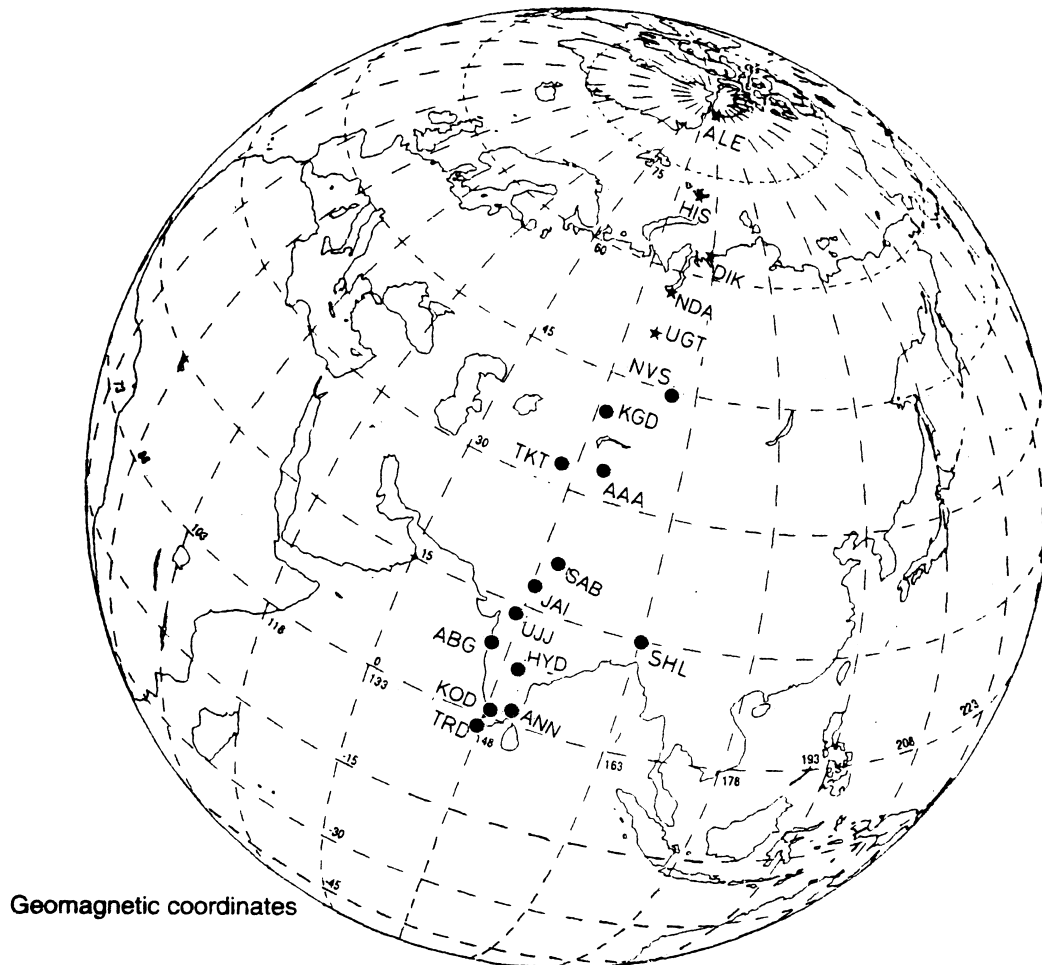**1975/77 Geomagnetic Observatories**

Fig. 1. Geographical location of the dense network of magnetic observatories that were operated during 1975 to 77. Data from the stations marked with "•" were considered for the present study. The dashed lines show the geomagnetic latitudes and longitudes in 15^0 steps.

2.   The Magnetic Data Base and Preparation of the Dataset for Analysis

The data base comprises daily mean values of the geo-magnetic D, H, and Z components for 901 days. These data were recorded at a network of 13 magnetic observatories which operated during the International Magnetospheric Study (IMS) period of 1975–77. All the observatories are confined to the 150^0 geomagnetic longitude band and extend from the dip equator to polar regions (Fig. 1). The selected epoch corresponds to a declining phase of solar activity, during which time the recurrence tendency of magnetic storms at 27-day intervals is well defined (Banks, 1969).

Following the procedure outlined in Schultz and Larsen (1983), the data were statistically corrected in the time domain for missing values, man-made errors and random noise (if any), before proceeding for further analysis. This statistical treatment has shown that in each data set, less than 2 to 3% of the data are outliers. Errors due to bad baseline values (evident as "step" or "box-car" functions in the magnetograms), etc. were rare.

Fluctuations in the intensity of an extra-terrestrial ring current encircling the Earth in the geomagnetic equatorial plane at a distance of a few Earth radii is the source for geomagnetic variations at periods of 27-day and its harmonics. The ring current spatial characteristics at the surface of the Earth can be represented in terms of a series of odd-degree zonal harmonics. Since the position of the ring current is controlled by the Earth's main magnetic field, and also since the P_1^0 zonal approximation is valid in the geomagnetic coordinate system, the geomagnetic reference frame is best suited for the analysis of long-period variations. Where the observatories are widely distributed over several longitude regions, it is always preferable to test the data *a priori*, whether they are confined to the geomagnetic reference frame or not, for induction studies at long periods. However, factors such as the proximity of a station to a nearby sea-coast, the presence of local (internal) electrical conductivity anomalies, or the presence of an external non-ring current source might also seriously contaminate the data with the result that the recorded field variations are no longer well expressed in the geomagnetic coordinate system. Although, the former is not the case in the present study, it is suspected that the strong influences of the latter might affect the data, particularly when large lateral conductivity contrasts are known to exist beneath the Indian region.

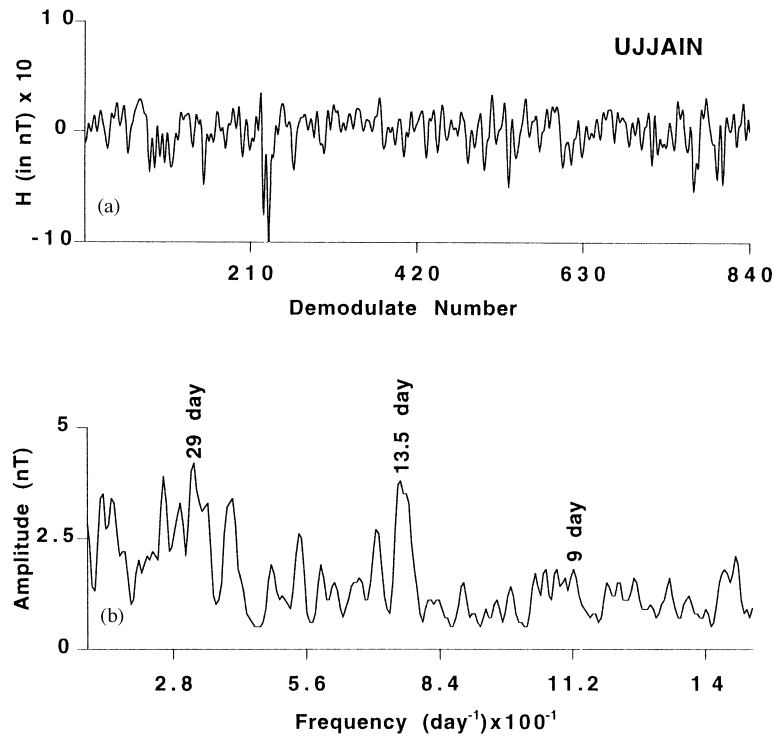To check for such effects, the data were subjected to a

Fig. 2. An example plot of (a) raw data plotted against its filtered number of data points and (b) its smoothed spectrum, plotted against frequency, for the *H* data of one of the stations, Ujjain (UJJ).

time-domain rotational transformation, following the procedure of Schultz and Larsen (1983). The obtained rotation angles are given in Table 1. It is seen from this table that the angles at all the stations are small, and comparable to their respective declination angles. This result suggests that the *preferred* plane, to which the data were transformed for their zonal nature, matches well with the geomagnetic co-ordinate system of the region in question, and thus the rotation angles agree well with the direction of the local dipole field (Schultz and Larsen, 1987; Banks and Ainsworth, 1992). Therefore, in the present analysis, only the un-rotated *H* data were utilized.

3. Time Series Analysis and Estimation of Complex Demodulates

Each time series of 901 days was subjected to a 30-point low-pass filter with a cut-off period of 4 days. The filtered data of length 841 points (after losing 30 points on either side of the original time series) were extended with zeros to 1728 ($= 2^6 \times 3^3$) to get optimum resolution of the required periodicities, centered at 27-day and its harmonics. The FFT spectra for the *H* component of all stations showed distinct peaks in the period bands of (*i*) 25–32, (*ii*) 11–16 and (*iii*) 8–10 days, representative of the 27-day period and its harmonics. An example of such a spectrum, plotted for one of the mid-latitude stations Ujjain (UJJ), is shown in Fig. 2. Next, the spectral estimates corresponding to these three period bands were subjected to complex demodulation (Banks, 1975). A total of 31 demodulate pairs (amplitude and phase), corresponding to the three period bands, were obtained for each station. The important aspect of the complex demodulation technique is that each demodulate, representing the *instantaneous* power level of the required frequency, can be treated as an independent entity and can be examined for source characteristics prior to estimating the EM response. In other words, the complex demodulation technique enables us to deal with the 'time-local' estimates of amplitude and phase for each cycle of the selected frequency in the data se-

Table 1. Angles obtained after applying the rotational transformation to X and Y data.

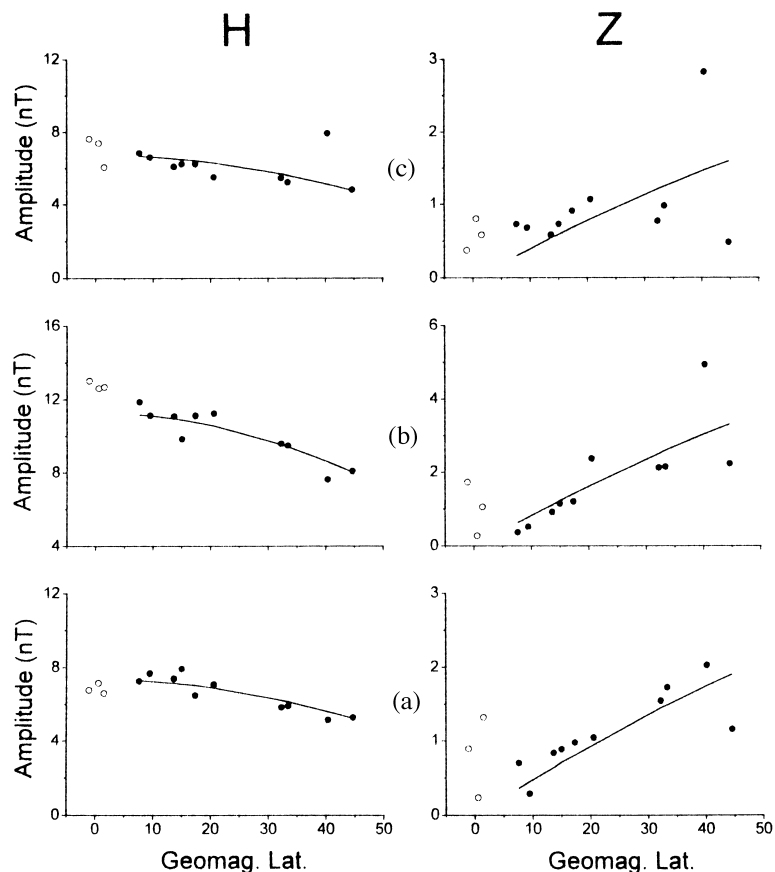| Station name	Code	Rotation angle (in degrees)	Declination (in degrees)
Trivandrum	TRD	−2.78	−2
Kodaikanal	KOD	−2.41	−2
Annamalainagar	ANN	−2.64	−2
Hyderabad	HYD	−1.63	−1
Alibag	ABG	−0.83	0
Ujjain	UJJ	−0.55	0
Shillong	SHL	−0.78	0
Jaipur	JAI	−0.81	0
Sabhawala	SAB	0.37	0
Tashkent	TKT	4.68	4
Alm-Ata	AAA	4.48	4
Karganda	KGD	8.25	8
Novosibirsk	NVS	8.54	8

Fig. 3. Best fit P_1^0 curves (solid lines) for a selected demodulate corresponding to (a) 25–32, (b) 11–16 and (c) 8–10 day period bands. The best fit is obtained in a least-squares sense, by considering only those stations represented by solid circles and by excluding the equatorial stations (open circles). Note the consistency in the P_1^0 representation of the H demodulates at all period bands, though there exists a pronounced scatter in Z at the higher harmonics of 27-day period. For the present analysis, equatorial stations (open circles) and auroral stations (not shown in the figure) have been excluded.

quence, rather than using the averaged amplitude over all the cycles, as practised in the FFT and other conventional spectral estimation methods. It is this special advantage of the method that makes it possible to statistically test the validity of each demodulate at a given station for zonal dependency, before using the demodulates for further analysis. Further mathematical and theoretical aspects of this technique, with applications, are described by Banks (1975). A lucid example of the application of this technique has also been given by Agarwal *et al.* (1980).

4. Test for $P_1^0 \cos(\theta)$ Dependence of the Inducing Source Field

In most of the earlier works, the validity of the P_1^0 approximation for the inducing field has been assumed, rather than demonstrated (for e.g., Pecova *et al.*, 1980; Petersons and Anderssen, 1990; Chen and Fung, 1991). In the present work, in view of the availability of continuous and uninterrupted data from the chosen observatory network (Fig. 1), it was possible to test the demodulates statistically, for the validity of their P_1^0 dependence. This statistical test has facilitated to identify some demodulates which did not satisfy the required P_1^0 criterion. Perhaps, these demodulates might be contaminated by external non-ring current (and hence nonzonal) sources or by some other factors. Recently, Arora (1999), by applying a principal component analysis tech-

nique to the same dataset used in the present study, has also studied the effect of non-zonal principal components on the reliability of the EM response at long periods. Thus, it is always preferable to identify those datasets, which can be defined as non-zonal in a statistical sense, and can be excluded from the analysis.

Figure 3 shows example plots of best-fit P_1^0 curves for a selected demodulate at all the stations, corresponding to 25–32 (3(a)), 11–16 (3(b)) and 8–10 (3(c)) day period bands. It is seen that the spatial characteristics of the H demodulates are well defined, and that a regional trend depicting source characteristics compatible with the P_1^0 term is consistent at all the period bands. While Z demodulates show a good P_1^0 consistency for 25–32 day period band (Fig. 3(a)), they show a pronounced scatter in 13.5 and 9 day periods (Figs. 3(b) and (c)). The scatter appears to increase with decreasing period, suggesting the influence of lateral inhomogeneities on the data at these higher harmonics. However, it was found that these effects (suspected as being due to lateral conductivity contrasts) were reduced by determining a band-averaged response, involving all the stations, for these two period bands. This procedure is discussed in the following section.

The presence of high conductivity zones and complex tectonic settings in the southern region of India (see figure 1 of Chandrasekhar and Arora, 1994), combined with the influence of the equatorial electrojet and predominant induc-

Table 2. Response estimates (depth (h*) and conductivity (σ) of the perfect substitute conductor) and their corresponding phases, obtained by a robust method for the stations shown in Fig. 4 for the period band of 25–32 days. The values given in the parentheses represent the errors associated with the respective estimates.

Station Name	h* (in km)	σ (S/m)	Phase
UJJ	$1362-515i$ (± 53)	0.60 (± 0.12)	-20.7^0 ($\pm 2.1^0$)
SHL	$1400-523i$ (± 62)	0.58 (± 0.14)	-20.5^0 ($\pm 2.4^0$)
JAI	$1315-341i$ (± 74)	1.36 (± 0.59)	-14.5^0 ($\pm 3.1^0$)
SAB	$1331-1062i$ (± 106)	0.14 (± 0.03)	-38.6^0 ($\pm 3.6^0$)
TKT	$1277-520i$ (± 51)	0.58 (± 0.12)	-22.2^0 ($\pm 2.1^0$)
AAA	$1029-703i$ (± 30)	0.32 (± 0.03)	-34.3^0 ($\pm 1.4^0$)

tion effects from the adjacent oceans, make the Z variations recorded at the equatorial stations TRD, KOD and ANN (open circles in Fig. 3), highly unreliable at all periods. Also, the nature of the Z demodulates is found to be anomalous at auroral latitude stations (not shown in Fig. 3), as evident by their significant deviation from the best P_1^0 fit. These features persist in all the demodulates of equatorial and auroral latitude stations, and thus the demodulates corresponding to these stations did not warrant their further usage in the analysis. The best fit P_1^0 curves (solid lines) in Fig. 3 were obtained without considering the equatorial (shown as open circles) and auroral stations.

5. Determination of C-response Functions
5.1 Single-station response

For determining the single-station response function, the Z and H demodulates corresponding to the 27-day period band were used, as only they showed good agreement with the expected zonal nature (as in Fig. 3(a)).

The univariate linear regression with the parameter $C(\omega)$, as a transfer function between $Z(\omega)$ and $H(\omega)$, is given by

$$Z(\omega) = C(\omega) \cdot H(\omega) + \delta Z(\omega) \qquad (1)$$

where $\delta Z(\omega)$ is the residual term in Z. $H(\omega)$ and $Z(\omega)$ represent H and Z at frequency ω, and are obtained by

$$H = \left| \frac{1}{r} \frac{\partial V}{\partial \theta} \right|_{r=R} \qquad (2)$$

$$Z = \left| \frac{\partial V}{\partial r} \right|_{r=R}. \qquad (3)$$

Here V is the magnetic scalar potential, defined for zonal harmonics as a function of geomagnetic co-latitude θ, by

$$V(r, \theta) = R \sum_n \left[e_n(\omega)(r/R)^n \right.$$
$$\left. + i_n(\omega)(R/r)^{n+1} \right] P_n(\cos \theta) \qquad (4)$$

and P_n is the Legendre function of degree n. R is the radius of the Earth. $e_n(\omega)$ and $i_n(\omega)$ respectively denote the external and internal parts of the field at ω. The least-squares solution for $C(\omega)$ is given by

$$C(\omega) = \left[\sum_{n}^{N} Z(\omega) \cdot H^*(\omega) / \sum_{n}^{N} H(\omega) \cdot H^*(\omega) \right] \qquad (5)$$

where "$*$" denotes the complex conjugate and N denotes the number of demodulates. $C(\omega)$ obtained by Eq. (5) is substituted in Eq. (1) to obtain the calculated $Z(\omega)$, $Z_{cal}(\omega)$. Then the error associated with $Z(\omega)$ is given by

$$\delta Z(\omega) = \left[\frac{1}{N-1} \sum^{N} (Z_{dif}(\omega))^2 \right]^{1/2} \qquad (6)$$

where $Z_{dif}(\omega) = Z(\omega) - Z_{cal}(\omega)$. The demodulates violating the condition

$$|Z_{dif}(\omega)| < |\delta Z(\omega)| \qquad (7)$$

are designated as outliers.

In the robust approach, the response is determined iteratively, by scaling the outliers (see Eq. (7)) with the "median" of the distribution of the real and imaginary parts of the residuals of the Z demodulates (Schmucker, 1998, pers. commn.), until the condition prescribed in Eq. (7) is satisfied.

5.1.1 Determination of error in $C(\omega)$ The error in Z which cannot be predicted by H is given by

$$< \delta Z Z^* > = \epsilon^2 < Z Z^* > \qquad (8)$$

where

$$\epsilon^2 = 1 - coh^2 \qquad (9)$$

and

$$coh^2 = \frac{| < Z H^* > |^2}{< Z Z^* > \cdot < H H^* >} \qquad (10)$$

"$<>$" denotes the average over the number of demodulates. coh^2 is the squared coherence between Z and H. If $(1-\beta)$ is the probability that the estimator $|C|$ lies within the range $[|C| - \Delta C, |C| + \Delta C]$, then ΔC, the error estimate of C is given by (Schmucker, 1999)

$$\Delta C^2 = |C|^2 \cdot \frac{\epsilon^2}{coh^2} \cdot \left[\left(\frac{1}{\beta} \right)^{1/m} - 1 \right] \qquad (11)$$

where $m = (\gamma - 2)/2$ can be found from the degrees of freedom γ ($= 2N$), of the averaging process. ΔC can be

Table 3.   Depth (h*) and the conductivity (σ) of the perfect substitute conductor for three different period bands, representing 27-day period and its harmonics. The values in the parentheses depict the corresponding error estimates.

Period band (days)	Weighted mean h* (km)	Weighted mean conductivity (S/m)
25–32	1177 (±191)	0.34 (±0.19)
11–16	900 (±101)	0.23 (±0.08)
8–10	825 (±296)	0.15 (±0.10)

treated equal for both Re(C) and Im(C). In the present computation, the errors have been calculated for $\beta=0.05$. i.e., for 95% confidence level.

The real (in-phase) part of the C-response (Re$C(\omega)$) gives the central depth (h*) of the induced currents, and the imaginary (out-of-phase) part (Im$C(\omega)$) yields, approximately, the conductivity (σ) at the penetration depth. The conductivity can be estimated by (Lilley and Sloane, 1976)

$$\sigma = \left[0.8\pi\omega(ImC(\omega))^2\right]^{-1}. \qquad (12)$$

Table 2 shows the response estimates and their corresponding phases, together with their respective error estimates obtained for individual sites, corresponding to the 25–32 day period band.

5.2   Band-averaged response

In determining the band-averaged response, first, the response for each individual Z-H demodulate pair of all the stations corresponding to each band was calculated using Eq. (5). That means, in this exercise, N in Eq. (5) denotes the total number of stations.

The obtained response was used to determine Z_{cal} values for each station for their subsequent error test shown in Eq. (7). If the Z demodulate of any station failed to meet the Eq. (7) criterion, then the response was recomputed, after rejecting that station's Z-H demodulate pair. This iterative procedure became necessary, for some demodulates corresponding to the 11–16 and 8–10 day period bands. Then using the responses of all the demodulates corresponding to each band, the band-averaged response was determined following the procedure of Beamish and Banks (1983). It is worthy of mention here that because of this averaging process, the effect of pronounced scatter of the demodulates corresponding to the 11–16 and 8–10 day period bands (Figs. 3(b) and (c)) was averaged out, leading to a reliable and meaningful band-averaged response at these higher harmonics of 27-day period.

Table 3 shows the band-averaged responses for the three period bands, together with their errors. The solid curve in Fig. 5(a) depicts these band-averaged responses.

6.   Discussion
6.1   Lateral variation in the depth of the conductosphere

The robust approach adopted in determining the single-station response has resulted in producing reliable response estimates for only 6 stations, viz., UJJ, SHL, JAI, SAB, TKT, AAA. These stations, all situated in the mid-latitude region, signify the fact that only they show consistency with a P_1^0 dependence of the inducing source (see Fig. 3(a)) as well

as with a local 1-D internal electrical structure of the Earth. This observation is consistent with those of Roberts (1986), Schultz and Larsen (1987), Banks and Ainsworth (1992) and many others.

It is seen from Table 2 that the responses at all the mid-latitude stations strictly satisfy the inequality criteria, viz., Re$C(\omega) > 0$ and Im$C(\omega) \leq 0$ prescribed by Weidelt (1972). Whittal and Oldenburg (1992) suggested that, for an EM response to represent a true conductosphere model, the phase of $C(\omega)$ (i.e., Arg($C(\omega)$)) should satisfy the condition $-\pi/4 < \text{Arg}(C(\omega)) < 0$. The derived responses at these 6 mid-latitude stations satisfy these conditions and thus they represent a reliable conductosphere model. Interestingly, the depth estimate at SAB is stable and matches well with those of the adjoining stations, particularly those situated south of SAB, although lateral inhomogeneities are known to exist near this station (for e.g., Nityananda et al., 1981) because of its close proximity to the Himalayan collision zone. Perhaps at SAB, the effect of near-surface lateral inhomogeneities could have been masked due to the induction at the long periods in question.

Figure 4 shows a contour plot of the conductosphere depths for the stations shown in Table 2. From this figure, it is seen
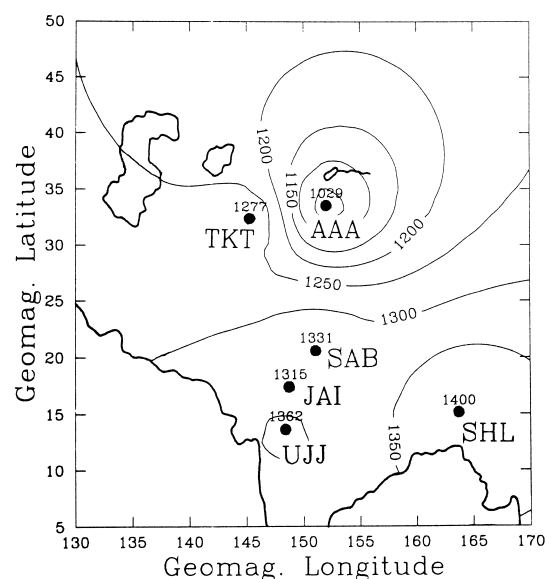

Fig. 4.   Contour plot of the conductosphere depth, h* (in km), for the period band of 25–32 days, for 6 mid-latitude stations (Table 3), whose response is compatible, both with the P_1^0 approximation of the inducing source, as well as with a local 1-D internal structure of the Earth.
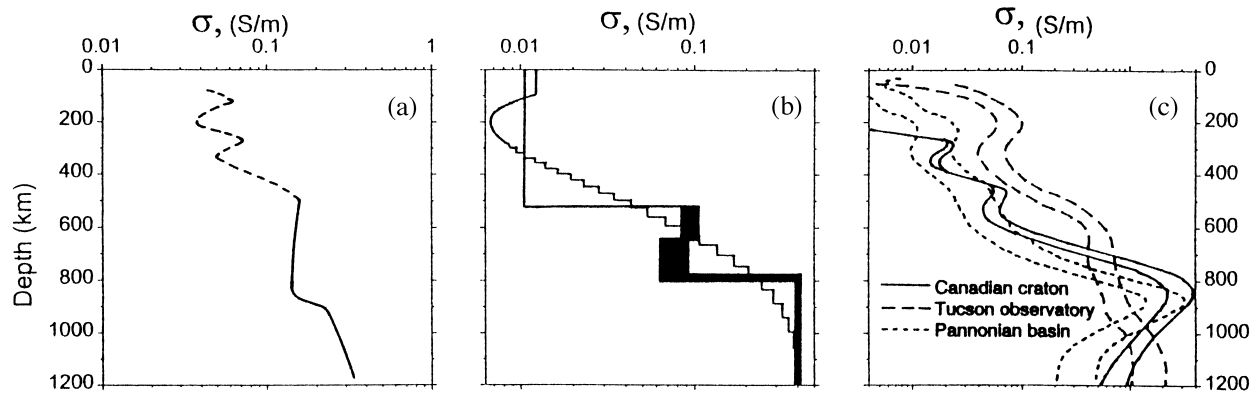
Fig. 5. Comparison of the geo-electrical structure of the mantle for (a) the Indian region, obtained by augmenting the Sq analysis results (dashed line) of Arora *et al.* (1995) with the present study (solid line), (b) the European region (after Olsen, 1998) and (c) the Pannonian basin, the North American region and the Canadian craton (Semenov *et al.*, 1997; Egbert and Booker, 1992; Schultz *et al.*, 1993). The conductivity increase at 850 km depth range, depicting the presence of a "mid-mantle conductor", which is clearly seen in all the regions, can be considered to be a global phenomenon.

that the depths at each individual station are similar, and give a mean depth range of about 1200 ($\pm$ 200) km for this region (Table 3). A relationship between conductosphere depths and latitude has earlier been reported for the European (Pecova *et al.*, 1980) and North American (Petersons and Anderssen, 1990) regions. While Petersons and Anderssen (1990) considered the decrease in depth of conductosphere with increase in latitude at any given period to be a characteristic of the real Earth, Pecova *et al.* (1980) attributed these gradients to be indicative of some deep E-W striking feature below central Europe. Though the depths obtained for the Indian region might first suggest a latitudinal dependence, the differences in the depth estimates are in fact negligible, when compared with the error estimates at individual sites, and so do not permit such an interpretation of these data for the Indian region.

Since the mid-latitude stations show convincingly their agreement with both a P_1^0 approximation and a 1-D internal electrical structure for 27-day period, these datasets could be analysed at further longer periods, for probing still greater depths beneath the Indian region. Such a study is under consideration.

6.2 Comparison of the derived conductivity-depth profile with other regional models

Figure 5 shows conductivity-depth profiles for the Indian region obtained by augmenting the Sq analysis results of Arora *et al.* (1995) with the band-averaged response of the present study (Fig. 5(a)), for the European region (Fig. 5(b)) and for the Pannonian basin and other regions (Fig. 5(c)). Arora *et al.* (1995) discussed the conductivity profile up to 500 km depth, derived from the analysis of Sq variations (the dashed line in Fig. 5(a)) utilizing the same data sets as used in the present study. Hence, only the geo-electrical profile corresponding to the periods of 27-day and its harmonics (the solid line in Fig. 5(a)) is discussed here, by comparing it with other regional models.

Geo-electrical structures of the lower mantle, obtained by combined magnetotelluric (MT) and magnetovariational responses in the Pannonian basin (Semenov *et al.*, 1997), by very long period MT response at Tucson observatory (Egbert and Booker, 1992) and for the Canadian craton (Schultz *et al.*, 1993), show an increased conductivity at 850 km depth

(Fig. 5(c)). However, the conductivity increase reported for Tucson observatory is not significant, when compared with that of other regions (as shown in the same plate, Fig. 5(c)). The EM response obtained by the combined analysis of Sq and geomagnetic storm-time variations for European region (Olsen, 1998) also shows a well-marked conductivity increase at around 800 km depth (Fig. 5(b)). Semenov *et al.* (1997) attribute this enhanced conductivity to be a manifestation of a mid-mantle conductor at 850 km. The present results (the solid line in Fig. 5(a)) also show a conductivity increase at the depth range of 800–900 km, between the 2nd and 3rd harmonics of 27-day period, corroborating this observation. Since these new evidences show that the electrical conductivity mapped in many regions has a pronounced increase at the depth range of 850 km, it may be surmised that the presence of a *mid-mantle conductor* at this depth range could be considered to be a global phenomenon. The main feature of such a mid-mantle conductor is that it is situated much deeper than the well-known 660-km seismic discontinuity, where the β–γ phase change is observed to produce a discontinuous conductivity change (Omura, 1991). (On this matter, the present data set could not resolve such a conductivity 'step' at 660 km because of the restricted frequency range in the data.) Another possibility would be to relate an electrical conductivity increase at 850 km with a 920-km seismic discontinuity, as reported by Kawakatsu and Niu (1994) for the Japanese islands.

7. Conclusions

Reliable single-station response estimates, consistent with a P_1^0 dependence of the source field and a local 1-D internal Earth structure, could be obtained for 6 stations, situated in the mid-latitude region along the Indo-Russian chain of stations (Fig. 1). The single-station response estimates were determined by a robust method after statistically testing the data for the validity of a P_1^0 approximation of the inducing source. Conductivity and depth estimates thus obtained are fairly constant, and do not demonstrate a variation in the depth of conductosphere as a function of latitude, as reported elsewhere. The mean depth of a perfect substitute conductor in Indian region is determined to be 1200 ($\pm$200) km, with an

average conductivity of 0.7 (±0.3) S/m. An increase in the estimated conductivity in the depth range of about 800–900 km may be due to the presence of a mid-mantle conductor, which can be considered to be a global phenomenon. A further study of still longer period variations of the 6 mid-latitude stations is under consideration.

References

Agarwal, A. K., B. P. Singh, and N. Nityananda, An application of complex demodulation technique to geomagnetic data and conductivity anomalies, *Proc. Indian. Acad. Sci.*, **89**, 67–77, 1980.

Arora, B. R., Electromagnetic response and source field characterisation from meridional chain of geomagnetic observatories, Abstract of XXII general Assembly of IUGG, Birmingham, UK, Abstracts volume of Week B, 324, 1999.

Arora, B. R., W. H. Campbell, and E. R. Schiffmacher, Upper mantle electrical conductivity in the Himalayan region, *J. Geomag. Geoelectr.*, **47**, 653–665, 1995.

Banks, R. J., Geomagnetic variations and the electrical conductivity of the upper mantle, *Geophys. J. Roy. Astr. Soc.*, **17**, 457–487, 1969.

Banks, R. J., Complex demodulation of geomagnetic data and the estimation of transfer function, *Geophys. J. Roy. Astr. Soc.*, **43**, 87–101, 1975.

Banks, R. J. and A. N. Ainsworth, Global induction and the spatial structure of mid-latitude geomagnetic variations, *Geophys. J. Int.*, **110**, 251–266, 1992.

Beamish, D. and R. J. Banks, Geomagnetic variations anomalies in northern England: Processing and presentation of data from a non-simultaneous array, *Geophys. J. Roy. Astr. Soc.*, **75**, 513–539, 1983.

Chandrasekhar, E. and B. R. Arora, Upper mantle electrical conductivity distribution beneath Indian subcontinent using geomagnetic storm time variations., *Mem. Geol. Soc. India*, **24**, 149–157, 1992.

Chandrasekhar, E. and B. R. Arora, On the source field geometry and geomagnetic induction in southern India, *J. Geomag. Geoelectr.*, **46**, 815–825, 1994.

Chandrasekhar, E. and B. R. Arora, Complex demodulation and electromagnetic response function for geomagnetic field variations at 27-day and its harmonics, *J. Assoc. Explr. Geophys.*, **XVII**, 91–98, 1996.

Chapman, S. and A. T. Price, The electrical and magnetic state of the interior of the Earth as inferred from terrestrial magnetic variations, *Phil. Trans. Roy. Soc. Lond.*, **A-229**, 427–460, 1930.

Chen, P. F. and P. C. W. Fung, Electromagnetic response function for the period of 27-day in Chinese region, *J. Geomag. Geoelectr.*, **43**, 979–987, 1991.

Egbert, G. D. and J. R. Booker, Very long period magnetotellurics at Tucson observatory: Implications for mantle conductivity, *J. Geophys. Res.*, **97**, 15099–15115, 1992.

Honkura, Y. and M. Matsushima, Electromagnetic response of the mantle to long-period geomagnetic variations over the globe, *Earth Planets Space*, **50**, 651–662, 1998.

Kawakatsu, H. and F. Niu, Seismic evidence for a 920-km discontinuity in the mantle, *Nature*, **371**, 301–305, 1994.

Lilley, F. E. M. and M. N. Sloane, On estimating electrical conductivity using gradient data from magnetometer arrays, *J. Geomag. Geoelectr.*, **28**, 321–328, 1976.

Nityananda, N., A. K. Agarwal, and B. P. Singh, An explanation of induced magnetic variations at Sabhawala, India, *Phys. Earth Planet. Int.*, **25**, 226–231, 1981.

Olsen, N., The electrical conductivity of the mantle beneath Europe derived from C-responses from 3 to 720 hr., *Geophys. J. Int.*, **133**, 298–308, 1998.

Omura, K., Change of electrical conductivity of olivine associated with olivine-spinel transition, *Phys. Earth Planet. Int.*, **65**, 292–307, 1991.

Pecova, J., K. Pec, and O. Praus, Remarks on spatial distribution of long period variations in the geomagnetic field over European area, in *Electromagnetic Induction in the Earth and Moon*, edited by U. Schmucker, pp. 171–186, Academic Publication, Japan, 1980.

Petersons, H. F. and R. S. Anderssen, On the spherical symmetry of the Electrical conductivity of the Earth's mantle, *J. Geomag. Geoelectr.*, **42**, 1309–1324, 1990.

Roberts, R. G., The deep electrical structure of the Earth, *Geophys. J. Roy. Astr. Soc.*, **85**, 583–600, 1986.

Schmucker, U., A spherical harmonic analysis of solar daily variations in the years 1964–1965: response estimates and source fields for global induction—II. Results, *Geophys. J. Int.*, **136**, 455–476, 1999.

Schultz, A. and J. C. Larsen, Analysis of zonal field morphology and data quality for a global set of magnetic observatory daily mean values, *J. Geomag. Geoelectr.*, **35**, 835–846, 1983.

Schultz, A. and J. C. Larsen, On the electrical conductivity of the mid-mantle: I. Calculation of equivalent scalar magnetotelluric response functions, *Geophys. J. Roy. Astr. Soc.*, **88**, 733–761, 1987.

Schultz, A., R. D. Kurtz, A. D. Chave, and A. G. Jones, Conductivity discontinuities in the upper mantle beneath a stable craton, *Geophys. Res. Lett.*, **20**, 2941–2944, 1993.

Semenov, V. Yu., A. Adam, M. Hvozdara, and V. Wesztergom, Geoelectrical structure of the Earth's mantle in Pannonian basin, *Acta Geod. Geoph. Mont. Hung.*, **32 (1-2)**, 151–168, 1997.

Weidelt, P., The inverse problem of geomagnetic induction, *J. Geophys.*, **38**, 257–289, 1972.

Whittal, K. P. and D. W. Oldenburg, Inversion of magnetotelluric data for a one dimensional conductivity, in *Geophys. Monogr. Ser., Soc. of Explr. Geophys.*, edited by D. V. Fitterman, **5**, 1–114, 1992.

E. Chandrasekhar (e-mail: esekhar@rcep.dpri.kyoto-u.ac.jp)